High resolution hyperspectral imagery to assess wheat grain protein in a farmer's field

Rodrigues Jr., F.A.[1]; Ortiz-Monasterio, I.[1]; Zarco-Tejada, P.J.[2]; Toledo, F.H.R.B.[1], Schulthess, U.[1]; Gérard, B.[1]

[1] International Maize and Wheat Improvement Center - CIMMYT, Texcoco, Mexico.

F.A.Rodrigues@cgiar.org

[2] Instituto de Agricultura Sostenible (IAS), Consejo Superior de Investigaciones Científicas (CSIC), Cordoba, Spain.

A paper from the Proceedings of the
13th International Conference on Precision Agriculture
July 31 – August 4, 2016
St. Louis, Missouri, USA

Abstract. The agricultural research sector is working to develop new technologies and management knowledge to sustainably increase food productivity, to ensure global food security and decrease poverty. Wheat is one of the most important crops into this scenario, being among the three most important cereal commodities produced worldwide. Precision Agriculture (PA) and specially Remote Sensing (RS) technologies have become in the recent years more affordable which has improved the availability and flexibility of acquiring images from both manned and unmanned vehicles. For this reason, CIMMYT's research agenda aims at developing new crop management practices using PA/RS technologies. As part of these efforts, a wheat experiment was established on a farmer's field in the Yaqui Valley, northwestern Mexico, sown in January and harvested in May 2014. This work focuses on the evaluation of narrow-band physiological spectral indices to estimate wheat grain protein content (GPC). Also to determine the optimum normalized difference spectral index (NDSI) and ratio spectral index (RSI), aiming to better explore the use of the hyperspectral signal on the assessment of GPC. A weekly/biweekly flight campaign took place from GS31 stage (stem elongation) until harvest, totaling 10 airborne images acquired at high resolution with a micro-hyperspectral imaging sensor ranging from 400-850 nm region, flying at 1200 m above ground resulting in a ground resolution of 1 m. Manual grain sampling took place just before harvest through a targeted grid of 14 sampling points on block A and a half regular / half stratified grid of 50 sampling

points each on block B. Under the conditions of this study, characterized by low spatial variability within the commercial field, the results obtained yielded coefficients of determination among vegetation indices (VIs) and GPC ranging from non-significant to 0.14 across all images. Complete two by two combinations of wavelengths approach applied into NDSI formula performed better on assessing GPC than VIs from the literature. However, the spectral region beyond the visible and near-infrared might be needed to assess GPC at field level. On the other hand, this approach allowed visualizing the spectral range/wavelengths that predominantly better explained GPC across the crop cycle than ordinary VIs.

Keywords. *narrow-band indices, normalized difference spectral index, ratio spectral index, spatial-temporal variability*

Introduction

Wheat is one of the three most important cereal commodities produced worldwide, after maize and rice. It is also one of the most important crops in Mexico, grown on more than 500,000 ha in 2012, with average yields of 3.2 Mt (FAO, 2015). Crop management is key to profitable and sustainable wheat production, which must be able to address with soil and climate spatial and temporal variability, aiming to improve grain yield and quality.

It is well known that there is spatial variability of yield and grain quality within a crop field due to soil spatial variability, weather conditions and crop management (Reyns et al., 2000; Stewart et al., 2002; Delin, 2004; Diacono et al., 2012). Although RS technologies show great potential to detect such variabilities within a crop cycle, there are only a few studies relating grain protein content with reflected electromagnetic radiation captured in satellite imagery (Basnet et al., 2003; Wright et al., 2004; Zhao et al., 2005; Feng et al., 2014; Wang et al., 2014) or low-altitude platform and proximal sensing (Hansen et al., 2002; Wang et al., 2004; Wright et al., 2004; Jensen et al., 2007; Li-Hong et al., 2007). The majority of these studies used just multispectral data.

RS technologies have become less expensive in recent years, which have improved the flexibility of acquiring images. The most commonly used VI is the Normalized Difference Vegetation Index (NDVI). It has been correlated with crop yield and quality (Mullan, 2012 and references therein). Although the results presented by those authors were considered useful, it is well documented that NDVI saturates at high leaf area index (LAI) values, and is also affected by other factors such as soil background, canopy shadows, illumination, atmospheric conditions and variation in leaf chlorophyll concentration (Zarco-Tejada et al., 2005a).

New methods that use hyperspectral remote sensing allow for the calculation of several other narrow-band VIs, suggested as potentially useful for PA (Willis et al., 1999; Zarco-Tejada et al., 2005a). Besides the VIs currently presented in the literature, hyperspectral signals can be used to calculate complete combinations of all available wavelengths using generic formulas, e.g. normalized difference spectral indices (NDSI) and ratio spectral indices (RSI), (Inoue et al., 2008a, 2008b; Stagakis et al., 2010; Inoue et al., 2012; Stratoulias et al., 2015). The present study examines the correlation between grain protein content (GPC) and narrow-band physiological spectral indices measured during the crop cycle in a wheat field and attempts to identify the optimum NDSIs and RSIs for the assessment of GPC. This approach allows to determine the consistency of VIs across a crop cycle, and shows possibilities on the prediction of potential areas of grain protein and also exploring possible different VIs across the spectrum.

Material and Methods

Field site and data collection

The experiment was carried out on a wheat field in the Yaqui Valley near Ciudad Obregón, (Sonora), in north-western Mexico (27°23'43.83"N and 109°55'0.90"W), during the 2014 wheat crop cycle. It consisted of two furrow irrigated blocks (called here ‘A’ and ‘B’) of 40 ha each, which were sown with the variety Cirno-C2008 in January 2014 and harvested at the end of May.

A weekly/biweekly flight campaign took place from GS31 stage (Zadoks et al., 1974) on 14th February until prior to harvest (07th May), resulting in 10 airborne images. They were acquired with a micro-hyperspectral imaging sensor (400-850 nm spectral region) flying at 1200 m above ground in a manned airplane, yielding a ground resolution of 1 m.

The micro-hyperspectral sensor was radiometrically calibrated in the laboratory using derived coefficients with a calibrated uniform light source (integrating sphere, CSTM-USS-2000C Uniform

Source System, LabSphere, NH, USA) at four levels of illumination and six integration times. Hyperspectral imagery was atmospherically corrected using the total incoming irradiance at 1 nm intervals simulated with the SMARTS model developed by the National Renewable Energy Laboratory, US Department of Energy (Gueymard, 1995, 2005) using aerosol optical depth measured at 550 nm with a Micro-Tops II sun photometer (Solar LIGHT Co., Philadelphia, PA, USA) collected in the study areas at the time of the flights. SMARTS computes clear sky spectral irradiance, including direct beam, circumsolar, hemispherical diffuse, and total on a tilted or horizontal plane for specified atmospheric conditions. The algorithms were developed to match the output from the MODTRAN complex band models within 2%, using aerosol optical depth as input. The spectral resolution is 0.5 nm for the 280–400 nm region, 1 nm for the 400–1750 nm spectral regions. This radiative transfer model has been previously used in other studies to perform the atmospheric correction of narrow-band multispectral imagery.

Manual grain sampling (Pask et al., 2012) took place just before harvest using a half regular / half stratified grid of 50 sampling points each in Block B (100 points in total), where 10% of the regular grid points were re-allocated in shorter distances than the original grid for a better variogram fitting. Each sampling point was based on 2 m^2 frame centered on the point geocoordinates, where all wheat plants were harvested, threshed and a grain sub-sample was taken for laboratory quality analysis. In Block A, there were 14 sampling points, which were selected based on a simple inspection of the soil apparent electrical conductivity (EC_a) map (Rodrigues Jr. el al, 2015), so that they covered the full range of variation of EC_a.

Data analysis

The grain protein content (GPC) data from Block B was interpolated onto 3 m grid (pixels of 9 m2) using global block kriging, fitting the best global variogram according to the spatial variability of the data. The purpose of GPC mapping is to visualize the within-field spatial variability. Map analysis and display were done using the ArcGIS software suite (v10.1; ESRI, Redlands, USA).

As a first step, the hyperspectral signal of each image was resampled into 7.5nm bandwidth to decrease noise effect, resulting in 58 wavelengths which were used for the subsequent analyses. Reflectance of the highest and lowest grain protein sampling point from each hyperspectral image were extracted and plotted. Afterwards, 41 different VIs ranging from chlorophyll, structural, red edge ratios and RGB indices (NDVI, RDVI, EVI, OSAVI, SR, MSR MTV1, MTV2, MCARI1, MCARI2 - Structural Indices; TVI, MCARI, TCARI, TCARI/OSAVI, MCARI/OSAVI, GM1, GM2, PSSRa, PSSRb, PSSRc, PSNDc - Chlorophyll Indices; ZMs - red edge ratios; Red, Green – RGB ratios; BG1, BG2, CAR, PRI515, PRI, PRIn, PRI*CI, PSRI, RARS, RNIR*CRI550, RNIR*CRI700, SIPI, VOG; (Zarco-Tejada et al., 2001, 2005a, 2005b, 2013 and references therein) were calculated using the necessary wavelengths (400-850 nm) from each hyperspectral image. These VIs were chosen based on their structural information as well as on their relationships with chlorophyll. Both, canopy structure and its greenness are indicators of the N-status of the plants.

The spectral information was extracted from each image using the point sampling location from both blocks (n=114). The extraction was done taking the average of a 3x3 window (9 m^2) around each sampling point. Linear regressions were calculated between the VIs and the GPC ($p \leq 0.05$). The coefficients of determination (R^2) were ordered into a decreased direction, aiming to identify the variables that showed higher correlations with GPC at each crop stage.

Afterwards, we applied two types of generic formulas aiming to generate spectral indices (SI) with a complete two by two combinations of spectral wavelengths, the ratio spectral index (RSI) and the normalized difference spectral index (NDSI). The RSI and NDSI are defined as:

$$RSI(i,j) = \frac{R_i}{R_j}\,;\; NDSI(i,j) = \frac{R_i - R_j}{R_i + R_j}$$

where *Ri* and *Rj* are the reflectance for wavelengths i and j respectively. Representation of RSI and

NDSI are the PSSRa (Blackburn, 1998) and NDVI (Rouse et al., 1974). Both use near-infrared and red wavelengths. Spectral indices using the complete two by two combinations of the hyperspectral signal were generated applying the RSI and NDSI formulas, similar to studies from Inoue et al., (2008a, 2008b); Stagakis et al., (2010); Inoue et al., (2012); Stratoulias et al., (2015).

Furthermore, regression analyses were done using RSI and NDSI indices as predictors for GPC. Maps of coefficient of determination (R^2) between these SI and GPC were generated to provide inclusive information of the optimum pair of wavelengths to assess GPC along the crop cycle (Inoue et al., 2008a, 2008b).

Results and Discussion

Grain protein content showed a distribution with mean and median values close to each other, reflecting broadly symmetrical (normal) distribution (Fig. 1) although with a high value of kurtosis.

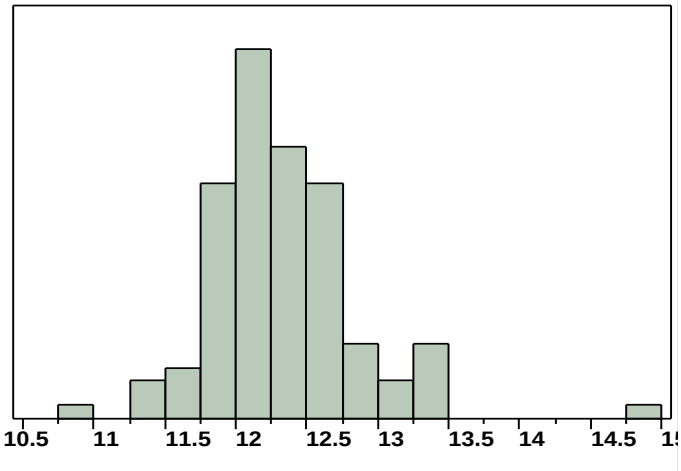

Maximum	14.96
3º Quartile	12.56
Median	12.25
2º Quartile	12.03
Minimum	10.87
Mean	12.32
Variance	0.26
Skewness	1.25
Kurtosis	5.67
CV	4.15

Figure 1 – Descriptive statistics for grain protein content (GPC - %).

Through the GPC mapping (Fig. 2) it is possible to visualize the within field spatial variability, which ranged from 10.8 to 14.9 %. The threshold of 12.5% had been chosen based on the farmer's recommendation. The highest and lowest GPC were identified from the protein map and were afterwards used as reference for extracting the reflectance from the images during the crop cycle.

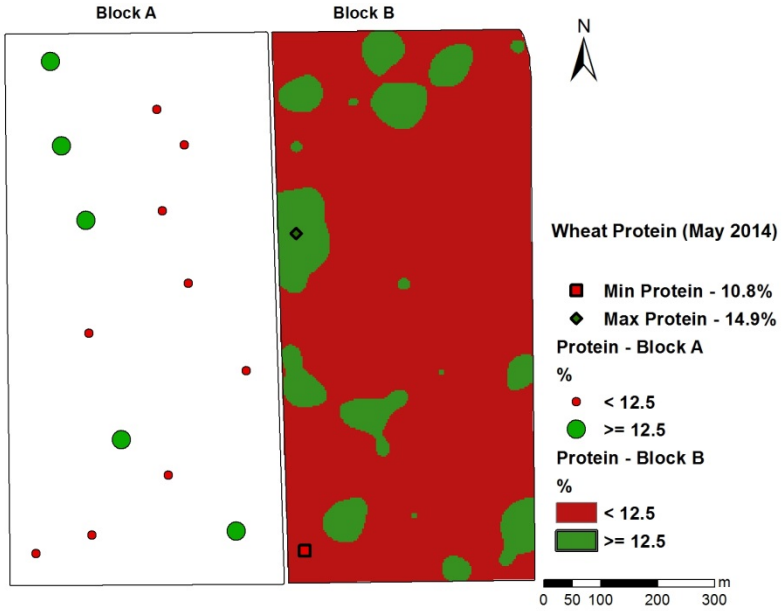

Figure 2 – Protein map.

The reflectance profile (Fig. 3a) from the highest (dashed lines) and lowest (full lines) grain protein region followed similar spectral behavior from 400 to 770 nm, with exception of the image from 25 April 2014 (around grain filling stage) which showed some difference in reflectance in the red region (around 680 nm) – more evident on Fig. 3b. At 840 nm (near infrared, NIR), it permitted to see some differences in the reflectance for the highest and lowest grain protein region.

The dark red dashed and full lines (14 Feb) represent the GS31 stage, which is an early stage for wheat where nutrient stress diagnosis may already be made. The darker green and pink (dashed and full) lines are from the beginning and end of anthesis, representing the peak of vegetation. At the early growth stage (GS31, 14 Feb – dark red lines), a small reflectance difference in the NIR region is detectable, the difference increases up to February 27, decreasing gradually until it reached the beginning of anthesis and then had a high difference again at the end of anthesis (07 April - pink lines, Fig. 3b).

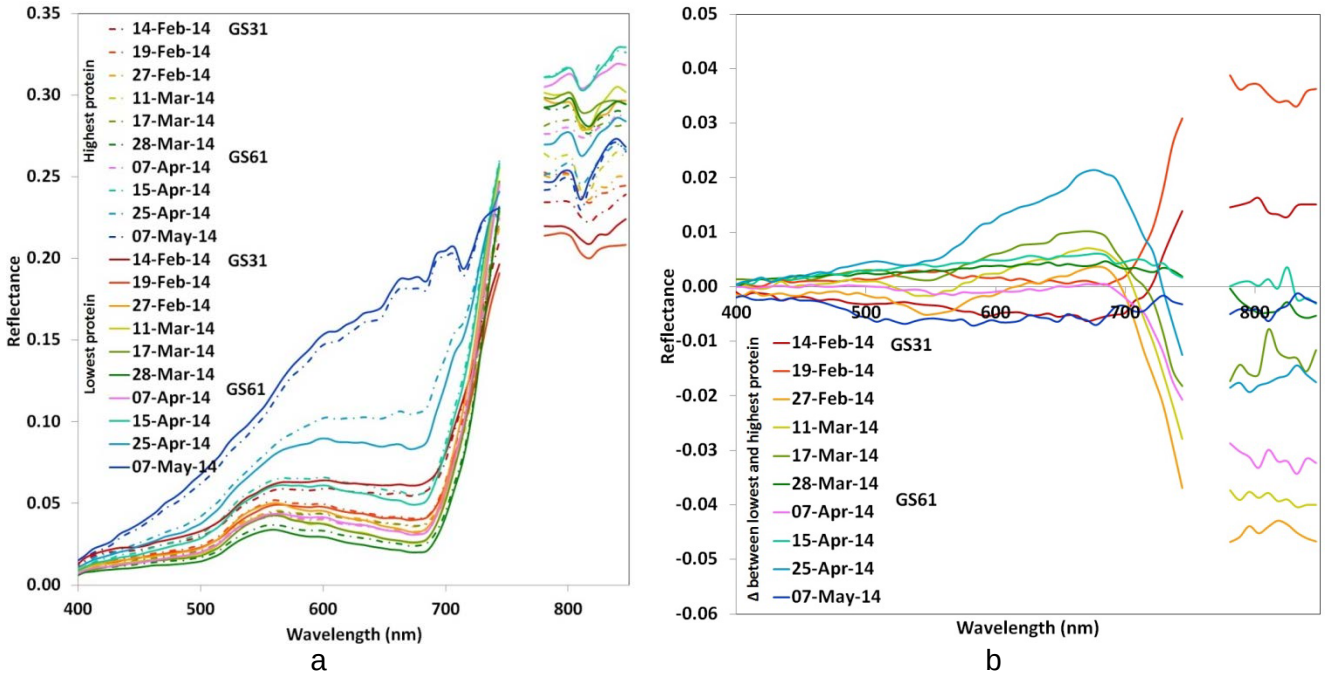

Figure 3 – Reflectance profile (a) and delta (b) from the highest and lowest GPC across crop cycle.

Zarco-Tejada et al. (2005a) found similar reflectance behavior for low and high growth areas of cotton. In the case of wheat, the best time to diagnose grain protein is around heading/anthesis stage as it corresponds to the time to increase grain protein through nitrogen management (Fischer et al., 1993). Therefore, identifying differences in reflectance at heading/anthesis time opens the possibility for nitrogen stress diagnosis while there is still time to raise grain protein through crop management.

Table 1 shows the best 10 R^2 for all images. Across the images, the R^2 ranged from non-significant to 0.14 (TVI from 27 February), changing the top VIs correlated to GPC across crop cycle, e.g. G in the first image (0.07), SR in the second (0.04), TVI in the third (0.14), and so on. Although specific VI with higher R^2 changed along the crop cycle, it is possible to claim the image date had bigger effect on describing GPC than the VIs per say. This affirmation is based on the range variation of top 10 R^2 within the same image, which did not vary much (e.g. 14 February – from 0.06-0.07).

Grain protein content is a function of the conversion of plant nitrogen content into protein (further reading in Mariotti et al. 2008), which could make us expect that leaf nitrogen concentration estimated through RS techniques may be able to partially explain grain protein content variation (Feng et al., 2014). Few studies reported the potential use of individual wavelengths and/or different VIs such as PPR (R550-R450/R550+R450), NDVI (R810-R680/R810+R680), RVI (R810/R680), GNDVI (R810-R560/R810+R560), GRVI (R810/R560) to describe nitrogen status and GPC (Hansen et al., 2002; Wang et al., 2004; Zhao et al., 2005; Li-Hong et al., 2007; Feng et al., 2014; Wang et al., 2014), all of them using VIs derived basically from green, red and NIR wavelengths into normalized and simple ratio formulas. NDVI, for instance, in our study was not part of the top 10 coefficients with GPC across the images and growth stages. However, the majority of those studies were carried out under controlled conditions, with different levels of nitrogen application. This may explain the rather low coefficients of determination observed in this study which was carried out on a farmer's field without treatments, resulting in a low range of variability.

In a further exploration from the hyperspectral signal, the RSI and NDSI formulas were applied to all possible combinations of the wavelengths – extracting the VIs calculated through this step and applying regression analysis using them individually as predictor variables for GPC. Since the results from the regression analysis using RSI and NDSI showed to be quite similar, just NDSI results are

shown here. The coefficient of determination (R^2) maps resulting from the regression analysis of the NDSI indices versus GPC are shown in Fig. 4.

Using the contour maps of R^2, it is possible to infer which wavelengths performed better when assessing GPC, being able to compare with R^2 from Table 1. The highest R^2 across the crop cycle were obtained in the images from 27 Feb – around booting stage (0.20 – R700, R574), 28 March - beginning of anthesis (0.18 – R515, R479) and 07 May 2014 - around ripening stage (0.21 – R707, R523). These values can be compared with the highest coefficients of VIs versus GPC from the same images (Table 1), with an R^2 of 0.14 for TVI (27 Feb), 0.03 for MCARI/OSAVI (28 Mar) and 0.11 for RARS (07 May), with an improvement on assessing GPC by NDSIs of up to 0.15 R^2 units. Although the complete two by two combinations of wavelengths improved the assessment to GPC, visible near-infrared (VNIR) may not be enough to assess GPC at field level

Through the contour maps it is also possible to visualize the wavelength region where R^2 were predominantly high, such as from 574 to 700nm on *Ri* and 400 to 574nm on *Rj* from 27 Feb – booting stage, strictly 515 to 530nm on *Ri* and specifically at 479nm on *Rj* from 28 March – anthesis and 707 to 840nm on *Ri* and 486 to 530nm on *Rj* – ripening stage; all of them showing slight R^2 differences once within those spectrum regions. This information is useful to decide about which sensor to use for measuring certain specific crop trait.

Table 1 – Best 10 coefficients of determination (R^2) between VIs and protein

Image - 14 Feb 2014		19 Feb 2014		27 Feb 2014		11 Mar 2014		17 Mar 2014		28 Mar 2014		07 April 2014		15 April 2014		25 April 2014		07 May 2014	
VIs	**Prot**	**VIs**	**Prot**	**VIs**	**Prot**	**VIs**	**Prot**	**VIs**	**Prot**	**VIs**	**Prot**	**VIs**	**Prot**	**VIs**	**Prot**	**VIs**	**Prot**	**VIs**	**Prot**
G	0.07	SR	0.04	TVI	0.14	TCARI/ OSAVI	0.10	MCARI	0.06	MCARI/ OSAVI	0.03*	MCARI /OSAVI	0.05	MCARI/ OSAVI	0.04	CAR	0.02*	RARS	0.11
SR	0.06	CI	0.04	MCARI 1	0.14	MCARI/ OSAVI	0.10	TCARI	0.06	TCARI/ OSAVI	0.03*	TCARI/ OSAVI	0.05	TCARI/ OSAVI	0.04	GM1	0.02*	PSND c	0.11
R750/R 670	0.06	GM2	0.04	MTVI1	0.14	TCARI	0.09	TCARI/ OSAVI	0.06	TCARI	0.02*	TCARI	0.03*	R710/ R700	0.02*	CI	0.02*	CAR	0.10
R710/R 670	0.06	R750/R7 00	0.04	PRIxCI	0.14	MCARI	0.09	MCARI/ OSAVI	0.06	MCARI	0.02*	MCARI	0.03*	PRI	0.02*	GM2	0.02*	PSSR c	0.10
PSSRa	0.06	R750/R6 70	0.04	EVI	0.13	PRIxCI	0.07	R700/ R670	0.05	PRI	0.01*	CAR	0.02*	MCARI	0.02*	R750/ R700	0.02*	RNIRx CRI70	0.08
PRIxCI	0.06	PSSRa	0.04	MCARI 2	0.13	MCARI 1	0.06	R710/ R670	0.04	R700/ R670	0.01*	CI	0.01*	TCARI	0.02*	RDVI	0.02*	RNIRx CRI55	0.07
MCARI 2	0.06	MCARI2	0.04	MTVI2	0.13	MTVI1	0.06	PRI	0.04	PRIn	0.00*	GM2	0.01*	GM2	0.02*	PRI	0.02*	PRI	0.07
MTVI2	0.06	MTVI2	0.04	RDVI	0.12	TVI	0.06	SR	0.04	PRIxCI	0.00*	R750/ R700	0.01*	R750/ R700	0.02*	EVI	0.02*	GM1	0.06
GM2	0.06	MCARI1	0.04	G	0.12	R710/ R670	0.06	G	0.04	R710/ R670	0.00*	GM1	0.01*	CI	0.02*	MCARI1	0.02*	SIPI	0.05
R750/R 700	0.06	MTVI1	0.04	R710/ R700	0.12	R700/ R670	0.06	R750/ R670	0.03	PSSRc	0.00*	PRIxCI	0.01*	CAR	0.01*	MTVI1	0.02*	MCAR I/OSA VI	0.04

* coefficients statistically NOT significant at 5% probability; Prot – Protein.

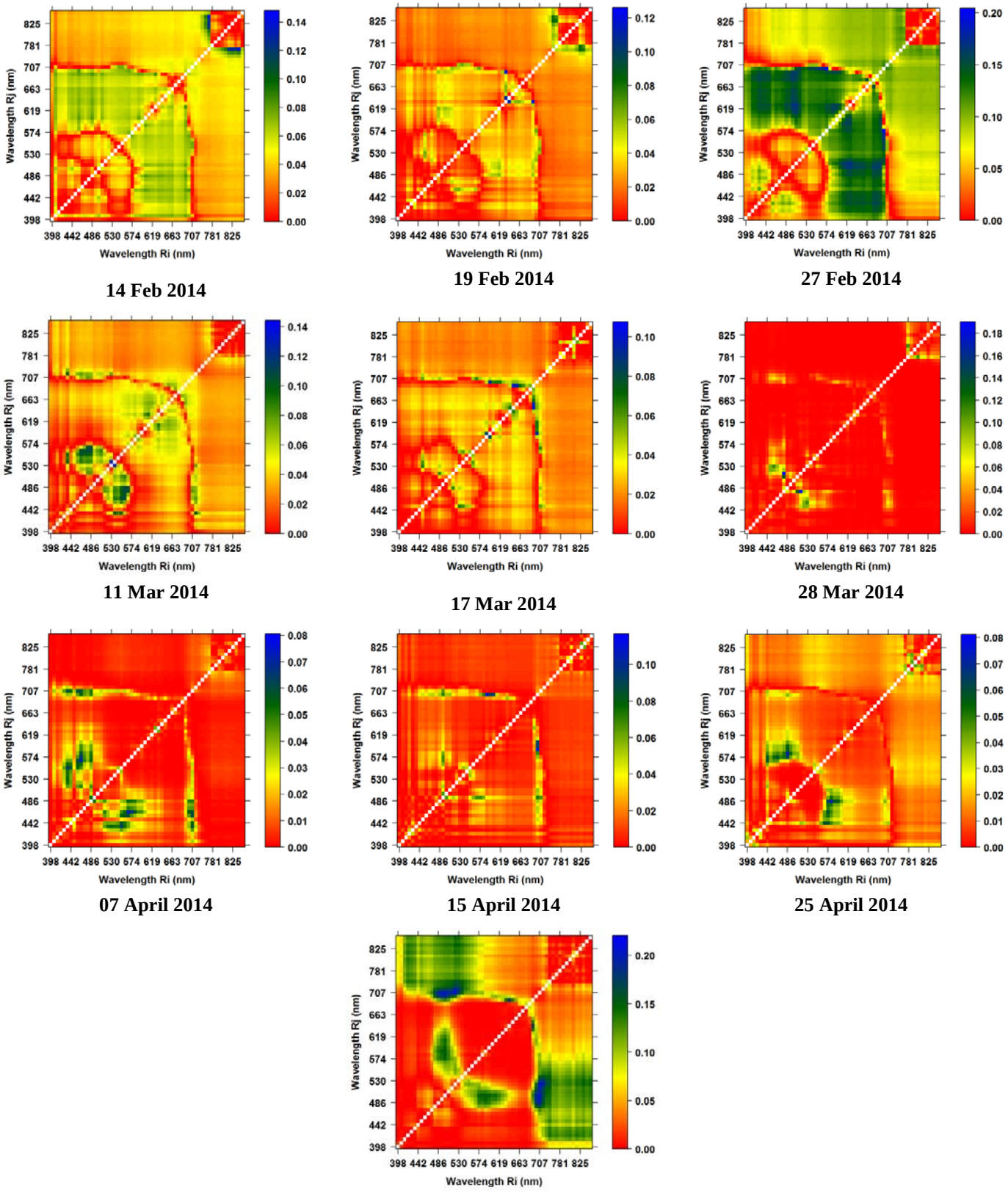

Figure 4 – Contour maps of the coefficient of determination (R^2) between NDSI (*Ri, Rj*) and GPC using the complete combinations of two wavelengths at i and j nm.

Those preliminary results showing low R^2s obtained between and VIs and GPC (Table 1) and NDSIs (Fig. 4) may be due to a non-linearity response, so further analyses should be done to check it. Furthermore, multivariate methods to join the best NDSI combinations along the crop cycle aiming at better assessment of GPC may also be considered. Another potential analysis would be to check how the complete two by two combinations approach can describe within yield variation and to apply cluster techniques to delineate management zones prior to harvesting.

Conclusion

The reflectance profile from the highest and lowest protein region followed similar spectral behavior from 400 to 770 nm, with exception of the image acquired during the grain filling stage, showing some difference on reflectance at the red region (around 680 nm). At 840 nm (NIR), it was possible to see small difference in the reflectance for the highest and lowest grain protein region at GS31 stage, increasing up to booting, and again at anthesis, giving support to further work for nutrient crop management to optimize grain protein through RS techniques.

Whilst it was possible to detect differences in reflectances, the coefficients of determination among VIs with GPC were in general weak across the crop cycle, which might be due to the lack of spatial variability within the commercial field used in this study. The top VIs varied for each image, and some image dates were more suitable to describe GPC.

Although the complete two by two combinations of wavelengths approach applied into NDSI formulae performed better on assessing GPC than VIs from the literature, VNIR may not be enough to assess GPC at field level, and additional assessments using the SWIR region might be needed. The approach reported in this paper allowed for visualizing the range of wavelengths within VNIR that predominantly better explained GPC across the crop cycle.

Acknowledgements

This work was funded partially by CIMMYT, under CRP Wheat and in part by the STARS project, an *integrated effort to improve our understanding of the use of remote sensing technology in monitoring smallholder farming*. See www.starsproject.org. We are very thankful to Jose Alberto Mendoza, Jose Urrea, Lorena González Pérez and the whole Crop Nutrition team for their assistance with the field measurements and flight campaign.

References

Basnet, B., Apan, A., Kelly, R., Jensen, T., Strong, W., Butler, D., 2003. Relating satellite imagery with grain protein content. In: Proceedings of the Spatial Sciences Conference, Canberra, Australia, pp. 22–27.

Blackburn, G. A. 1998. Spectral indices for estimating photosynthetic pigment concentrations: a test using senescent tree leaves. Int. J. Remote Sens. 19: 657-675.

CIMMYT, 2014. Global Conservation Agriculture Research. http://www.cimmyt.org/en/what-we-do/conservation-agriculture (Accessed Jan 2015).

Delin, S. 2004. Within-field variations in grain protein content: Relationships to yield and soil nitrogen and consistency in maps between years. Precision Agriculture, 5, 565–577.

Diacono, M., Castrignanò, A., Troccoli, A., De Benedetto, D., Basso, B., Rubino, P. 2012. Spatial and temporal variability of wheat grain yield and quality in a Mediterranean environment: A multivariate geostatistical approach. Field Crops Research, 131, 49-62.

FAO, 2015. FAOSTAT. http://faostat3.fao.org/faostat-gateway/go/to/home/E (Accessed February 2015).

Feng, M-c., Xiao, L-j., Zhang, M-j., Yang, W-d., Ding, G-w. 2014. Integrating Remote Sensing and

GIS for Prediction of Winter Wheat (Triticum aestivum) Protein Contents in Linfen (Shanxi), China. PLoS ONE, 9, e80989.

Fischer, R.A., Howe, G.N., Ibrahim, Z.1993. Irrigated spring wheat and timing and amount of nitrogen fertilizer. I. Grain yield and protein content. Field Crops Research, 33, 37.

Gueymard, C.A. 1995. SMARTS, A Simple Model of the Atmospheric Radiative Transfer of Sunshine: algorithms and performance assessment. Technical Report No. FSEC-PF-270-95. Florida Solar Energy Center, Cocoa, FL.

Gueymard, C.A. 2005. Interdisciplinary applications of a versatile spectral solar irradiance model: a review. Energy 30:1551–1576

Hansen, P.M., Jørgensen, J.R., Thomsen, A., 2002. Predicting grain yield and protein content in winter wheat and spring barley using repeated canopy reflectance measurements and partial least squares regression. Journal of Agriculture Science, 139, 307–318.

Inoue, Y., Miah, G., Sakaiya, E., Nakano, K., Kawamura, K. 2008a. NDSI map and IPLS using hyperspectral data for assessment of plant and ecosystem variables. Journal of the Remote Sensing Society of Japan, 28, 1–14.

Inoue, Y., Peñuelas, J., Miyata, A., Mano, M. 2008b. Normalized difference spectral indices for estimating photosynthetic efficiency and capacity at a canopy scale derived from hyperspectral and CO2 flux measurements in rice. Remote Sensing of Environment, 112, 156–172.

Inoue, Y., Sakaiya, E., Zhu, Y., Takahashi, W. 2012. Diagnostic mapping of canopy nitrogen content in rice based on hyperspectral measurements. Remote Sensing of Environment, 126, 210-221.

Jensen, T., Apan, A., Young, F., Zeller, L. 2007. Detecting the attributes of a wheat crop using digital 3D imagery acquired from a low-altitude platform. Computers and Electronics in Agriculture, 59, 66-77.

Li-Hong, X., Wei-Xing, C., Lin-Zhang, Y. 2007. Predicting grain yield and protein content in winter wheat at different N supply levels using canopy reflectance spectra. Pedosphere, 17, 646-653.

Mariotti, F., Tom, D., Mirand, P. P. 2008. Converting Nitrogen into Protein—Beyond 6.25 and Jones' Factors, Critical Reviews in Food Science and Nutrition, 48:2, 177-184, DOI: 10.1080/10408390701279749

Mullan, D. 2012. Spectral Radiometry. In: M.P. Reynolds, A. Pask and D. Mullan (Editors), Physiological Breeding I: Interdisciplinary Approaches to Improve Crop Adaptation. CIMMYT, INT., Mexico, D.F.

Pask, A.J.D., Pietragalla, J., Mullan, D.M., Reynolds, M.P. (Eds.) 2012. Physiological Breeding II: A field Guide to Wheat Phenotyping. Mexico, D.F.: CIMMYT.

Reyns, P., Spaepen, P., De Baerdemaeker, J. 2000. Site-Specific relationship between grain quality and yield. Precision Agriculture, 2, 231-246.

Rodrigues Jr., F. A., Ortiz-Monasterio, I., Zarco-Tejada, P. J., Schulthess, U., Gérard, B. 2015. High resolution remote and proximal sensing to assess low and high yield areas in a wheat field. In: Proceedings of the European Conference on Precision Agriculture, 10th conference, ECPA, Tel Aviv, Israel.

Rouse, J. W., Haas, R. H., Schell, J. A., Deering, D. W., Harlan, J. C. 1974. Monitoring the vernal advancements and retrogradation of natural vegetation. NASA/GSFC, Greenbelt, MD.

Stagakis, S., Markos, N., Sykioti, O., & Kyparissis, A. 2010. Monitoring canopy biophysical and biochemical parameters in ecosystem scale using satellite hyperspectral imagery: An application on a Phlomis fruticosa Mediterranean ecosystem using multiangular CHRIS/PROBA observations. Remote Sensing of Environment, 114, 977–994.

Stewart, C. M., McBratney, A. B., Skerritt, J. H. 2002. Site-Specific durum wheat quality and its relationship to soil properties in a single field in northern new south wales. Precision Agriculture, 3, 155-168.

Stratoulias, D., Balzter, H., Zlinszky, A., Tóth, V. R. 2015. Assessment of ecophysiology of lake shore reed vegetation based on chlorophyll fluorescence, field spectroscopy and hyperspectral airborne imagery. Remote sensing of environment, 157, 72-84.

Wang, L., Tian, Y., Yao, X., Zhu, Y., Cao, W. 2014. Predicting grain yield and protein content in wheat by fusing multi-sensor and multi-temporal remote-sensing images. Field Crops Research, 164, 178-188.

Wang, Z. J., Wang, J. H., Liu, L. Y., Huang, W. J., Zhao, C. J., Wang, C. Z. 2004. Prediction of grain protein content in winter wheat (Triticum aestivum L.) using plant pigment ratio (PPR). Field Crops Research, 90, 311-321.

Willis, P. R., Carter, P. G., Johansen, C. J. 1999. Assessing yield parameters by remote sensing techniques. p. 1413–1422. In: P.C. Robert et al. (ed.) Precision agriculture. Proceedings of the International Conference, 4th,. ASA, CSSA, and SSSA, Madison, WI, USA.

Wright, D. L., Rasmussen, V. P., Ramsey, R. D., Baker, D. J. 2004. Canopy reflectance estimation of wheat nitrogen content for grain protein management. GIScience and Remote Sensing, 4, 287-300.

Zadoks, J. C., Chang, T. T., Konzak, C. F. 1974. A Decimal Code for the Growth Stages of Cereals, Weed Research, 14:415-421.

Zarco-Tejada, P.J., Miller, J.R., Mohammed, G.H., Noland, T.L., Sampson, P.H. 2001. Scaling-up and model inversion methods with narrow-band optical indices for chlorophyll content estimation in closed forest canopies with hyperspectral data. IEEE Transactions Geoscience and Remote Sensing, 39(7):1491–1507.

Zarco-Tejada, P. J., Berjón, A., López-Lozano, R., Miller, J. R., Marin, P., Cachorro, V., et al. 2005b. Assessing vineyard condition with hyperspectral indices: Leaf and canopy reflectance simulation in a row-structured discontinuous canopy. Remote Sensing of Environment, 99, 271–287.

Zarco-Tejada, P.J., Ustin, S.L., Whiting, M.L. 2005a. Temporal and Spatial relationships between within-field yield variability in cotton and high-spatial hyperspectral remote sensing imagery. Agronomy Journal, 97(3):641-653.

Zarco-Tejada, P.J., González-Dugo, V., Williams, L.E., Suárez, L., Berni, J.A.J., Goldhamer, D., Fereres, E. 2013.A PRI-based water stress index combining structural and chlorophyll effects: assessment using diurnal narrow-band airborne imagery and the CWSI thermal index. Remote Sensing of Environment, 138, 38-50.

Zhao, C., Liu, L., Wang, J., Huang, W., Song, X., Li, C. 2005. Predicting grain protein content of winter wheat using remote sensing data based on nitrogen status and water stress. International Journal of Applied Earth Observation and Geoinformation, 7, 1-9.